

Experimental and theoretical conformational studies of hydrazine derivatives bearing a chromene scaffold

Nadezhda V. Markova ^a, Marin I. Rogojerov ^a, Violina T. Angelova ^b, Nikolay G. Vassilev ^{a,*}

^a Institute of Organic Chemistry with Centre of Phytochemistry, Bulgarian Academy of Sciences, Acad. G. Bonchev Str. Bl. 9, 1113, Sofia, Bulgaria

^b Department of Chemistry, Faculty of Pharmacy, Medical University - Sofia, 1000, Sofia, Bulgaria

ARTICLE INFO

Article history:

Received 25 April 2019

Received in revised form

10 July 2019

Accepted 31 July 2019

Available online 1 August 2019

Keywords:

Benzohydrazides

ab initio and DFT methods

Dynamic NMR

Conformational study

ABSTRACT

A conformational study of two novel hydrazine derivatives bearing a chromene moiety was carried out using *ab initio* and DFT quantum chemical methods, dynamic NMR and IR spectroscopy. The theoretical calculations predict and the experimental NOESY spectra confirm the (*E*)-*anti,anti* conformation as the most stable one in solution for the compounds (*N'*-[(*E*)-(2-methyl-2*H*-1-benzopyran-3-yl)methylidene]benzohydrazide and 4-hydroxy-*N'*-[(*E*)-(2-methyl-2*H*-1-benzopyran-3-yl)methylidene]benzohydrazide). The barriers of rotation around the amide bond in the studied compounds, ΔG^\ddagger , are in the range of 14.8–15.9 kcal mol⁻¹ and were reproduced very well by the DFT calculations at the SMD/B3LYP/6-31+G(d,p) level of theory. The GIAO ¹H and ¹³C chemical shifts calculated in DMSO and chloroform are in very good agreement with the experimental NMR data.

© 2019 Elsevier B.V. All rights reserved.

1. Introduction

Hydrazide–hydrazones constitute a class of organic compounds, which attracts the attention of medicinal chemists due to the fact that they contain an azomethine group (–NH–N=CH–) connected with a carbonyl group, and this makes them suitable for different pharmaceutical applications and makes possible the synthesis of different heterocyclic scaffolds [1], like 1,3,4-oxadiazolines [2], azetidin-2-ones [3], coumarins [4], 1,3-thiazolidin-4-ones [7], and 1,3-benzothiazin-4-ones [5]. Hydrazide–hydrazone derivatives are present in many bioactive molecules and display a wide variety of biological activities, such as antibacterial, antitubercular, antifungal, anticancer, anti-inflammatory, anticonvulsant, antiviral, and antiprotozoal action [6]. In recent years a number of hydrazide–hydrazone derivatives have been developed as antitubercular agents [7]. Our results, obtained from the evaluation of the biological activity of a series of coumarin and 2*H*-chromene and coumarin based hydrazones, show that some of them are potent antimycobacterial agents [8] and possess antioxidant, antiproliferative [9] and anticonvulsant activities [10,11].

Complete knowledge of the structure, including stereochemistry, is essential for lead optimization in drug discovery. Recently

Lopes et al. [12] studied the signal duplication in the ¹H- and ¹³C NMR spectra of *N*-acylhydrazone derivatives. The duplicated signals observed in NMR spectra of 4-methyl-2-phenylpyrimidine-*N*-acylhydrazone correspond to the presence of two CO–NH bond-related *syn* and *antiperiplanar* conformers.

A recent X-ray analysis of two hydrazide–hydrazone derivatives clarified their structure in solid state [8], but their behavior in solution is important when the compounds have drug potential. Therefore, the aim of this research is to elucidate the structure and conformational behavior in solution of two novel hydrazine derivatives bearing a chromene moiety, which recently demonstrated antimycobacterial [8] and antiproliferative activity [9], utilizing experimental NMR and IR spectral methods as well as theoretical calculations using *ab initio* and DFT quantum chemical methods.

2. Experimental

Chemicals and solvents were either purchased puriss p. a. from commercial suppliers or purified by standard techniques.

2.1. Synthesis of *N'*-[(*E*)-(2-methyl-2*H*-chromen-3-yl)methylidene]benzohydrazide (1**) and *N'*-[(*E*)-(2-methyl-2*H*-chromen-3-yl)methylidene]pyridine-4-carbohydrazide (**2**)**

The synthesis of the studied compounds **1** and **2** was described in a previous paper [9].

* Corresponding author.

E-mail address: niki@orgchm.bas.bg (N.G. Vassilev).

2.2. Characterization

For IR spectral measurements 8 wt % solutions of studied compounds were prepared in solvents CDCl_3 and $\text{DMSO}-d_6$. All IR spectra of target solutions were recorded on a *Tensor 27 Bruker FTIR spectrometer* in the $4000\text{--}500\text{ cm}^{-1}$ spectral region, accumulated by 64 scans with resolution of 2 cm^{-1} using a $100\text{ }\mu\text{m}$ path length NaCl liquid cell.

All NMR experiments were carried out on a Bruker Avance spectrometer II+600 MHz at $20\text{ }^\circ\text{C}$ in CDCl_3 and $\text{DMSO}-d_6$ as a solvent, using tetramethylsilane (TMS) as an internal standard. The precise assignment of the ^1H and ^{13}C NMR spectra was accomplished by measurement of 2D homonuclear correlation (COSY), DEPT-135 and NOESY, 2D inverse detected heteronuclear (C–H) correlations (HMQC and HMBC).

2.3. Computational details

All calculations were carried out using GAUSSIAN 09 program package [13] with default optimization criteria.

The geometries and normal mode vibrational frequencies of the rotamers of the two compounds **1** and **2** were computed by Density Functional Theory (DFT). Geometry optimization of these structures was carried out by the hybrid B3LYP functional which combines the three-parameter exchange functional of Becke [14] with the LYP correlation one [15] using 6-31 + G(d,p) basis set. The optimization at MP2/6-31 + G(d,p) level of theory was performed on the two most stable conformers according to B3LYP results. Frequency calculations at the same levels of theory were carried out for all the isomers reported in the study to determine whether the optimized structures were local minima or transition states (TSs) on the potential energy surface and to estimate thermal corrections.

Solvent effects (CDCl_3 and DMSO) for all studied isomers were taken into account by using the solvation model SMD (solvation model density) of Truhlar and co-workers [16] at SMD/B3LYP/6-31+G(d,p) level. The two most stable isomers embedded in conductor polarizable continuum, C-PCM formalism [17] at C-PCM/MP2/6-31 + G(d,p) level of theory were explored. SMD and C-PCM formalisms [17] were used to simulate the solvent effects as implemented in GAUSSIAN 09 [18].

The transition state structures obtained by rotation around the amide bond were localized at B3LYP/6-31+G(d,p) level of theory. The isomer geometries were optimized again in solvent medium at the same computational level (SMD/B3LYP/6-31+G(d,p)).

The Gibbs free energy, G , for all structures was obtained as the sum: $G = E_t + E_{\text{corr}}$, where E_t is the total (electronic + nuclear) energy and E_{corr} – thermal correction. For the calculation of the zero-point vibrational energies and thermal correction to total energy, the frequencies were retained unscaled. The values of Gibbs free energies (ΔG) and barriers ΔH^\ddagger , ΔS^\ddagger and ΔG^\ddagger were calculated at temperature 298.15 K.

Because of the sensitivity of ^{13}C NMR chemical shifts to the presence of polarization and diffuse functions in the basis set the 6-31+G(2d,p) basis set was employed. The proton and carbon isotropic shielding constants were calculated with the B3LYP functional using the gauge-including atomic orbitals (GIAO) approach [19,20] and C-PCM/MP2/6-31+G(d,p) optimized geometry. Incorporation of the solvent as dielectric into GIAO NMR calculations was used to estimate the effect of the medium (CDCl_3 and DMSO) on the chemical shifts of compounds **1** and **2**. In order to compare the theoretical data with the experimental ones, the calculated isotropic shielding constants, σ_i , were transformed to chemical shifts using the reference compound tetramethylsilane (TMS): $\delta_i = \sigma_i(\text{TMS}) - \sigma_i$, where both $\sigma_i(\text{TMS})$ and σ_i were calculated at

the same computational level, C-PCM/B3LYP/6-31+G(2d,p)//C-PCM/MP2/6-31+G(d,p).

2.4. Dynamic NMR studies

VT ^1H NMR spectra of compounds **1** and **2** were recorded on a Bruker II+ 600 instrument (BBO probe) at 600.13 MHz in steps of 10 K in CDCl_3 . Temperature calibration was done with B-VT 3000 unit (it was checked and calibrated with methanol and ethylene glycol reference samples). ^1H NMR spectra were acquired using a spectral width of 10 kHz, an acquisition time of 3.4 s and 32 scans, zero-filled to 64k datapoints (0.15 Hz per point) and processed without apodization.

The VT ^1H EXSY NMR spectra of compounds **1** and **2** were recorded on a Bruker II+ 600 instrument (BBO probe). The spectra were acquired using a spectral width of 0.8 kHz, 2048×256 complex time domain datapoints, with 2 scans in about 48 min. Linear prediction (32 coefficients and 256 points) in F1 was applied. The spectra were zero-filled to 1024×1024 datapoints and processed with a shifted square sine bell apodization in both dimensions. Populations and exchange rates were obtained from diagonal- and crosspeak integrals using EXSYCalc [21]. The program EXSYCalc does a quantitative analysis of the experimental intensities of the NMR peaks in EXSY experiments to calculate the exchange rates [22,23]. An alternative program for quantitative analysis of experimental intensities in EXSY spectra is D2DNMR [24].

The errors E_{tot} , quoted in Table 4 are calculated according to the expression: $E_{\text{tot}} = \sqrt{E_S^2 + E_{KT}^2}$, where E_S is the statistical error based on scattering of the data in the Eyring plot while E_{KT} is computed using error propagation equations as derived by Binsch in [25] and Heinzer and Oth [26], in which errors due to both the calculated rate constants and the measured temperature are taken into account. The absolute error in temperature is assumed to be not more than $\pm 0.5\text{ K}$. The relative errors in k are estimated to be not more than $\pm 10\%$ at all temperatures according to the precision of the volume integration of peaks. The errors analysis was performed using a proprietary computer program using the cited equations.

3. Results and discussion

3.1. Conformational analysis and molecular geometry

In order to obtain additional information on the structure of the compounds presented, a conformational analysis and geometry optimizations in the gas phase and solution (chloroform and DMSO) were carried out using DFT and *ab initio* calculations. As a starting point, the three dihedral angles shown in Fig. 1 were considered. Taking into account two possible values for each of the three dihedral angles defined in Fig. 1 and 0° (syn) and 180° (anti), the combinations give 8 distinct conformations (Scheme 1).

Quantum chemical calculations at B3LYP/6-31+G(d,p) and MP2/6-31+G(d,p) levels of theory using recently obtained X-ray

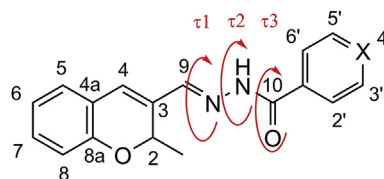
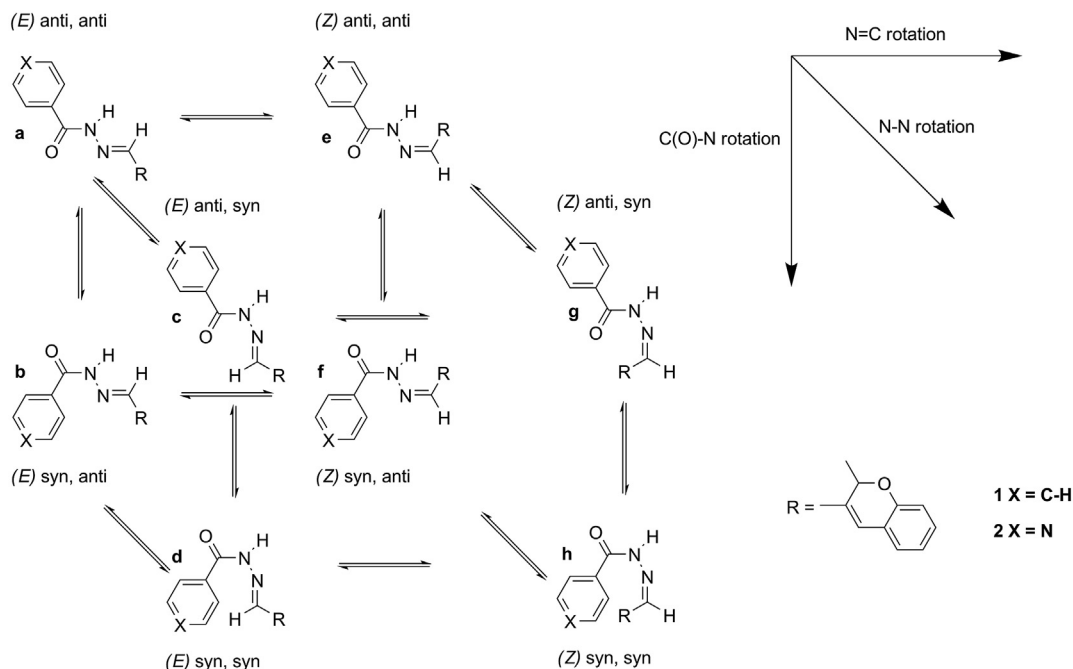


Fig. 1. Structural formula and atom numbering of the investigated compounds (**1**: $\text{X} = \text{CH}$, **2**: $\text{X} = \text{N}$). Rotation angles which are important in the conformational analysis are denoted as: τ_1 (C3-C9-N-NH), τ_2 (C9=N-NH-C10) and τ_3 (N-NH-C10=O).



Scheme 1. Possible stereoisomers and conformers of compounds **1** and **2**.

geometries [8] of compounds **1** and **2** were performed. The X-ray analysis showed the (*E*)-*anti,anti* (*a*) conformation in solid state. To investigate the conformational behavior of all eight conformations in gas phase and solution the theoretical studies were carried out.

Starting from structure *a* rotation around the amide C–N bond (angle τ_3) produces *syn, antiperiplanar* conformer *b* (Scheme 1). The rotation around the C=N bond (angle τ_1) is responsible for *Z* isomer *e*. The rotation around the N–N bond (angle τ_2) produces *anti, synperiplanar* conformer *c* of compounds **1** and **2**. When the rotation is around angle τ_1 in structures *b*, *c* and *e* the isomers *d*, *f* and *g* can form, respectively. Rotation around angle τ_3 in molecule *g* leads to forming of isomer *h*. The rotation around the three angles τ_1 , τ_2 and τ_3 in the different species can result in the formation of different isomers by successive reversible conversion.

The B3LYP/6-31+G(d,p) optimized structures of all stereoisomers of compounds **1** and **2** are presented in Fig. 2.

The free Gibbs energies and relative stabilities of the eight conformers (*a*–*h*) of compounds **1** and **2** are given in Table 1. In gas phase the most stable structure is isomer *b* of compound **1** and following in stability are isomers *c* (0.22 kcal mol^{−1}) and *b* (0.93 kcal mol^{−1}). The picture is similar for compound **2** – the most stable structure is isomer *b* followed by *c* (0.34 kcal mol^{−1}) and *a* (1.05 kcal mol^{−1}). According to our DFT calculations, conformers **1**(*d*–*h*) and **2**(*d*–*h*) are unstable structures. The energy differences were calculated to be in the range from 6 to 14 kcal mol^{−1} and the isomers *d*–*h* of the two compounds were not further considered in our analysis.

When the solvent effect was accounted for at SMD/B3LYP/6-31+G(d,p) level the most stable isomer becomes the species *a* for both compounds. The structure *b* is the next stable by energy. The free Gibbs energy difference in CDCl₃ between *a* and *b* is 0.95 kcal mol^{−1} for **1** and 0.37 kcal mol^{−1} for **2**. Isomer *c* is less stable by 2.51–2.23 kcal mol^{−1} relative to *a*. When DMSO was accounted for as solvent the free energy difference between *a* and *b* increases – 2.11 kcal mol^{−1} and 1.68 kcal mol^{−1} for compounds **1** and **2**, respectively.

The most stable structures, *a* and *b* of compounds **1** and **2** are optimized in gas phase, CDCl₃ and DMSO at MP2/6-31+G(d,p) level

of theory, as well. The isomers **1b** and **2b** are the more stable structures in gas phase and in solution. The energy difference between the two isomers is largest in gas phase – 2.65 kcal mol^{−1} and 2.88 kcal mol^{−1} for **1** and **2**, respectively. When the solvent is taken into account at C-PCM/MP2/6-31+G(d,p) level of theory the free energy difference significantly decreases for **1**–1.44 kcal mol^{−1} in dimethyl sulfoxide and 1.84 kcal mol^{−1} in chloroform. In the case of compound **2** the energy differences between the two forms are similar to compound **1**.

The analysis of the data in Table 1 shows that the inclusion of $\Delta ZPE^\#$ and $T\Delta S^\#$ terms at B3LYP and MP2 levels in gas phase and in solution does not lead to significant change in energy differences between the two forms of the compounds.

On the basis of the energy difference between the two isomers in the gas phase and solution it can be concluded that both forms should be present.

Differences between DFT and MP2 in predicting the most significant conformations of molecular systems have been reported by some authors [27,28]. It is generally accepted that the commonly used functionals of electron density, such as B3LYP, tend to underestimate dispersion effects which may play a role in the conformational stability of aromatic organic molecules. A comparison of the results obtained by the different electronic structure methods employed is also included in order to investigate the relevance of both correlation and dispersion effects in the conformer energies [29].

In order to facilitate the assignment of the experimental NMR spectra of the studied compounds in terms of different conformers in equilibrium, GIAO ¹H and ¹³C chemical shifts (δ /ppm) in DMSO and chloroform of the most stable conformers of compounds **1** and **2** were calculated at C-PCM//B3LYP/6-31+G(2d,p) level. As is seen from Table 2 the calculated GIAO ¹³C chemical shifts predict very well the experimental NMR data. However the calculated proton and carbon chemical shifts of conformers *a* and *b* are very similar and close to the experimental values, thus it is impossible to distinguish which conformer is the preferred one in solution only from GIAO calculations.

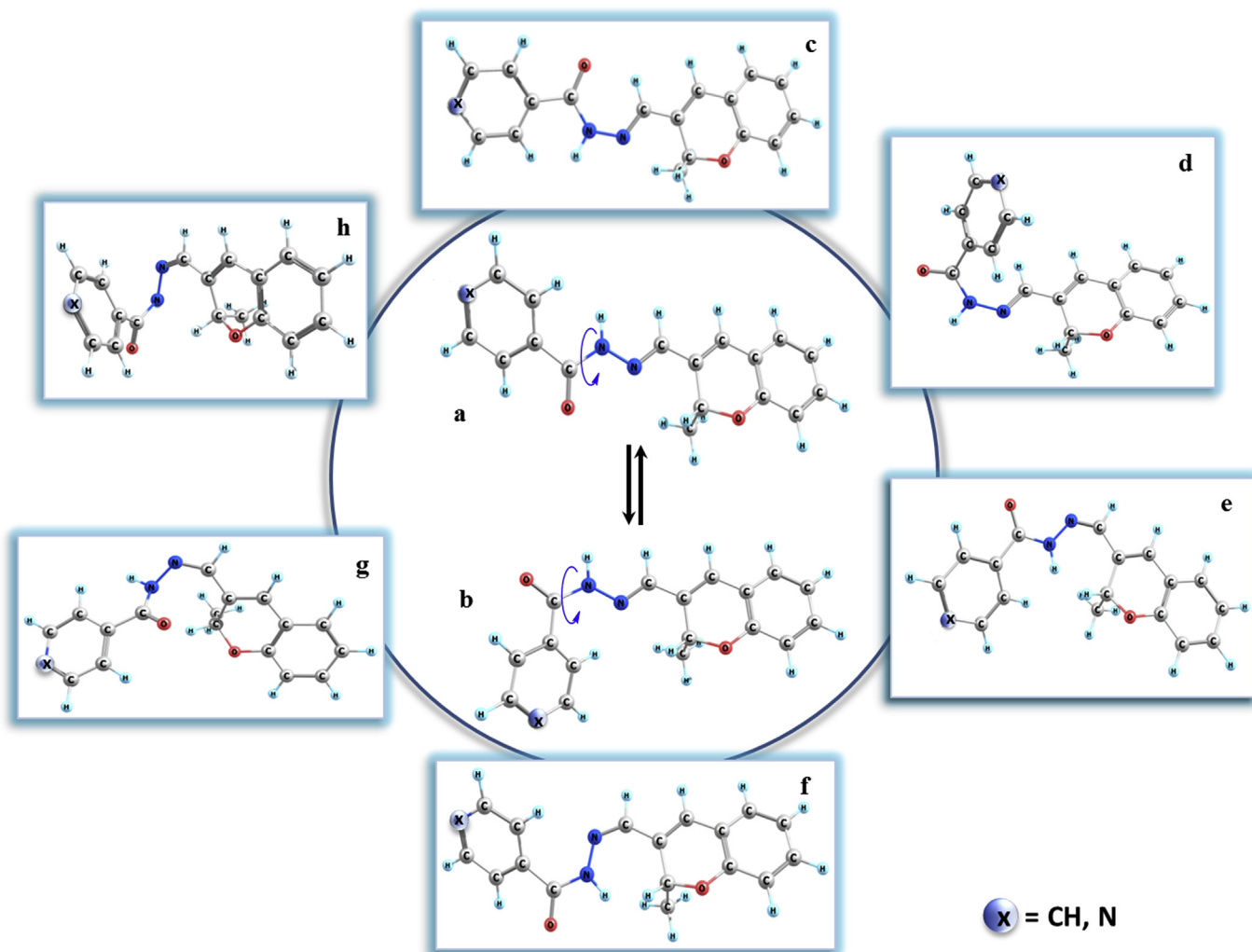


Fig. 2. B3LYP/6-31+G(d,p) optimized structures of the stereoisomers and conformers of compounds **1** and **2**.

3.2. IR analysis

The IR assigned characteristic frequency bands of compounds **1** and **2** in CDCl_3 and $\text{DMSO}-d_6$ are summarized in Table 3.

According to results of the *ab initio* and DFT calculations, several stereoisomers and conformers of **1** and **2** in gas phase and solution can be observed (see Scheme 1 and Fig. 2). This implies an amide CO–NH bond rotation and a coexistence of *syn/anti*periplanar conformers in solution has to be experimentally identified. Therefore major conformers **1a**, **2a** (as *(E)*-*anti,anti* (notation **a**)) and minor conformers **1b**, **2b** as *(E)*-*syn, anti* (notation **b**) should be detected in IR or NMR spectra measured in CDCl_3 and $\text{DMSO}-d_6$ solutions.

We have to note in advance, that the *anti* CO–NH group exhibits two characteristic bands: amide (I) at 1650 cm^{-1} and amide (II) at 1550 cm^{-1} . The geometrical structure of the *syn* (notation **b**) conformation does not allow the strong interaction between the $\nu(\text{NCO})$ and $\delta(\text{NH})$ vibrations characteristic of the *anti* (notation **a**) conformation, and thus the *syn* CO–NH group shows only the amide (I) band [30]. Hence, two amide (I) and one amide (II) bands could be observed in the IR spectra of the conformers of **1** and **2** in solution. It must also be pointed out that the band position of the *anti* amide group is considerably different from that of the *syn* amide group in IR spectrum. The NH stretching frequency of the

monomeric *anti* amide group lies $20\text{--}40\text{ cm}^{-1}$ higher than that of the *syn* amide group, and can be used as a diagnostic tool for *syn* and *anti* conformation recognition [31].

As it was mentioned above, the other source of *syn/anti*periplanar conformers (notation **a**, **c** and **d**, **f**) (see Scheme 1 and Fig. 2) is a hindered rotation around the N–N bond. It is obvious that the carbonyl-hydrazone ($-\text{C}=\text{N}-\text{NH}-\text{CO}-$) system force field changes in this type of rotation, especially as there should be a change in the conjugation between the amide $\text{N}-\text{C}=\text{O}$ and the $\text{C}=\text{N}$ bonds. This structural change would also lead to a frequencies shift in the amide (I) and amide (II) bands of **a** and **c** conformers as well as a similar alteration in the positions of the amide (I) bands of **d** and **f** conformers. Since **c**, **d** and **f** conformers are not more stable than **a** and **b** it is unlikely that the related bands will appear in the IR spectrum.

Finally, the $\text{C}=\text{N}$ double bond isomerization, assuming *E/Z* exchange around $\text{C}=\text{N}$ double bond, is likely probable since the energy difference between two isomers is large enough as shown by the *ab initio* calculations in gas phase and in solution (see results in part 3.1).

3.2.1. IR data of compound **1** in CDCl_3

Most likely, a small amount of water (H_2O) is released into the solution when dissolving **1** in CDCl_3 (practically 7–8% saturated

Table 1

Relative energies, ΔE_t , ΔH^0 and ΔG_{298} (kcal mol⁻¹) for the isomers of compounds **1** and **2** (Fig. 2) in the gas phase and in solution, calculated at B3LYP/6-31+G(d,p) and MP2/6-31+G(d,p) levels.

Species	B3LYP/6-31+G(d,p)			SMD/B3LYP/6-31+G(d,p)					
	gas phase			in DMSO			in CHCl ₃		
	ΔE_t	ΔH^0	ΔG_{298}	ΔE_t	ΔH^0	ΔG_{298}	ΔE_t	ΔH^0	ΔG_{298}
1a	1.40	0.96	0.93	0.00	0.00	0.00	0.00	0.00	0.00
1b	0.28	0.00	0.00	1.62	1.79	2.11	0.79	0.84	0.95
1c	0.00	0.10	0.22	3.25	3.69	4.16	1.58	2.07	2.51
1d	6.41	6.21	6.29	8.71	8.69	8.92	7.53	7.46	7.13
1e	10.78	10.52	10.06	8.09	8.85	9.77	8.57	9.29	10.06
1f	8.04	8.02	8.15	9.09	9.68	10.47	8.32	8.97	9.94
1g	10.19	10.43	10.49	10.76	11.51	12.32	10.20	10.94	11.37
1h	14.49	14.42	14.48	9.33	9.68	10.10	8.56	9.02	9.65
2a	1.34	1.14	1.05	0.00	0.00	0.00	0.00	0.00	0.00
2b	0.03	0.00	0.00	1.38	1.33	1.68	0.54	0.45	0.37
2c	0.00	0.33	0.34	3.37	3.63	3.71	1.67	1.97	2.23
2d	6.36	6.36	6.38	8.51	8.25	7.92	7.39	7.12	6.67
2e	10.68	10.33	10.20	8.09	8.34	8.53	8.64	9.09	9.26
2f	7.69	7.92	8.00	8.91	9.31	10.17	8.07	8.48	9.09
2g	10.12	10.57	10.54	10.81	11.20	11.46	10.21	10.83	11.26
2h	14.03	14.18	13.96	9.15	9.32	9.55	8.29	8.50	8.89
	MP2/6-31+G(d,p)			C-PCM/MP2/6-31+G(d,p)					
	gas phase			in DMSO			in CHCl ₃		
	ΔE_t	ΔH^0	ΔG_{298}	ΔE_t	ΔH^0	ΔG_{298}	ΔE_t	ΔH^0	ΔG_{298}
1a	2.80	2.78	2.65	1.59	1.57	1.44	1.99	1.97	1.84
1b	0.00	0.00	0.00	0.00	0.00	0.00	0.00	0.00	0.00
2a	3.08	3.01	2.88	1.65	1.58	1.45	2.21	2.14	2.01
2b	0.00	0.00	0.00	0.00	0.00	0.00	0.00	0.00	0.00

Table 2

GIAO¹³C chemical shifts (δ /ppm) in DMSO and chloroform of the most stable conformers of compounds **1** and **2** (bold for conformer *a* and in brackets for conformer *b*) calculated at C-PCM/B3LYP/6-31+G(2d,p) level and experimental data. The geometries are optimized at the C-PCM/MP2/6-31+G(d,p) level in DMSO and chloroform.

Nuclei	DMSO		Chloroform	
	1	2	1	2
C2	69.7	69.7	70.4	70.3
	75.1 (74.9)	74.9 (74.9)	74.9 (74.6)	74.7 (74.5)
C3	133.5	133.2	133.3	132.4
	134.7 (135.1)	134.3 (134.6)	135.1 (135.1)	134.5 (134.6)
C4	127.6	128.5	129.0	129.2
	132.7 (128.9)	134.0 (129.8)	131.5 (128.2)	132.7 (129.6)
C4a	121.4	121.4	121.3	121.1
	123.2 (125.1)	123.7 (125.2)	123.0 (124.8)	122.7 (123.2)
C5	127.6	127.8	127.4	127.6
	128.0 (127.6)	128.3 (128.2)	127.3 (124.8)	127.5 (127.4)
C6	121.5	121.6	121.2	121.4
	121.4 (121.9)	121.6 (121.9)	120.9 (121.4)	121.0 (120.8)
C7	130.7	131.0	130.9	131.3
	131.1 (129.6)	131.5 (129.8)	130.7 (129.3)	131.1 (129.7)
C8	116.5	116.5	117.0	117.0
	116.9 (117.8)	117.0 (118.1)	116.9 (117.8)	117.0 (117.6)
C8a	152.2	152.3	153.1	152.8
	154.2 (152.8)	153.6 (152.7)	154.3 (152.9)	154.6 (153.4)
C9	146.5	147.7	147.3	148.7
	148.0 (143.6)	149.7 (144.7)	146.5 (142.3)	147.7 (143.4)
C10	163.1	161.6	164.0	168.1
	167.7 (174.6)	166.6 (167.0)	166.8 (174.0)	165.6 (171.7)
C1'	133.4	140.5	133.1	140.4
	134.6 (135.3)	141.4 (141.3)	134.8 (135.2)	141.3 (140.0)
C2'	127.6	121.6	127.2	123.4
	127.9 (129.1)	121.8 (123.4)	127.6 (129.0)	121.2 (123.1)
C3'	128.5	150.4	128.8	150.7
	127.9 (127.7)	151.2 (151.2)	127.5 (127.2)	150.9 (150.9)
C4'	131.8	—	132.1	—
	131.9 (130.3)	—	131.2 (129.7)	—
CH ₃	19.3	19.3	19.5	19.5
	19.8 (19.7)	19.8 (19.9)	19.6 (19.6)	19.6 (19.8)

CDCl₃ solution was prepared). We should note that the crystallographic data show an intermolecular H-bonded chain between H₂O and molecule **1** [8]. Probably, the intermolecular H-bond is retained by dissolving **1** in CDCl₃ and a H₂O molecule is coordinated with **1a** or **1b**. In support of such an argument is the observed frequency band of $\nu(\text{O—H})$ stretching modes at 3620 cm⁻¹ which does not exclude the existence of dimeric forms in the solution (see Fig. 7S in supplementary). This suggestion can be proved by the presence in the IR spectrum of OH-bands typical for intermolecular H-bonded systems (3200–3100 cm⁻¹).

The carbonyl C=O amide (I) band is a complex multiplet (there are more than two overlapped bands) where the low frequency one at 1647 cm⁻¹ and a high frequency shoulder at 1676 cm⁻¹ could be assigned to both stable conformers **a** and **b**. A similar picture is observed in the high frequency region, where the N—H frequency $\nu(\text{N—H})$ at 3444 cm⁻¹ is probably not H-bonded, but the other observed at 3226 cm⁻¹ can be assigned to a H-bonded $\nu(\text{N—H})$ stretching vibration. However, we should note that this spectral interpretation of amide related bands in a context of two conformers **a** and **b** is quite complicated since there exist intermolecular hydrogen bonds between **1** and H₂O (small residuals in the solvent). Recent X-ray crystallographic data indicate such intermolecular hydrogen bonding interactions including H₂O (alcohol) molecules [8].

3.2.2. IR data of compound **1** in DMSO-*d*₆

A high frequency shift is observed in the carbonyl spectral region of **1** in DMSO-*d*₆ solution, where a C=O stretching frequency can be found at 1676 cm⁻¹ (compare IR spectra of Fig. 7S and 8S). A low frequency shoulder at 1647 cm⁻¹ cannot be clearly observed.

The presence of the expected doublet in the carbonyl region would be a certain indication for coexistence of both conformers **a** and **b** in solution. However, this picture is complicated by a breakdown of the molecular association with H₂O in DMSO-*d*₆ solution. Most probably, there is a formation of intermolecular hydrogen bond between N—H (of HC=N—NH—CO— group) and S=O (of DMSO-*d*₆). We should note that the frequencies $\nu(\text{N—H})$ at 3381 and 3195 cm⁻¹ suggest such a H-bonded system (**1** and DMSO-*d*₆).

3.2.3. IR frequency data of compound **2** in CDCl₃

The situation is quite similar with compound **2**. Most likely, a small amount of alcohol (C₂H₅OH) is released into the solution when dissolving the substance **2** in CDCl₃. The stretching vibration of C=N group $\nu(\text{C=N})$ can be assigned at 1608 cm⁻¹ (characteristic for hydrazones) and that of conjugated double bond $\nu(\text{C=C})$ was found at 1626 cm⁻¹ (see Table 3). These two bands should be doubled in the presence of two conformers, but that can hardly be shown in the IR spectrum due to a strong band overlap in this region (Fig. 9S).

Carbonyl C=O amide (I) band frequency can be found at 1647 cm⁻¹, having a high frequency shoulder at 1680 cm⁻¹, while the $\nu(\text{N—H})$ frequency at 3430 cm⁻¹ is most probably not H-bonded (see Table 3). The doublet in the carbonyl region might be interpreted as a result of the presence of both conformers **2a** and **2b**. However these observations can be complicated by a breakdown of the molecular association with alcohol in CDCl₃ solution. However, the observed frequencies at 3306 and 3180 cm⁻¹ can be assigned to a H-bonded $\nu(\text{N—H})$ stretching vibration, which suggests the existence of intermolecular hydrogen bonds between conformers of **2** and alcohol.

3.2.4. IR data of compound **2** in DMSO-*d*₆

A carbonyl C=O stretching frequency band of **2** observed at 1681 cm⁻¹ in DMSO-*d*₆ solution can be assigned to the **2a**

Table 3
Selected experimental and C-PCM/MP2/6-31+G(d,p) calculated frequencies (in cm^{-1}) of characteristic stretching modes found in IR spectra of compounds **1** and **2** and their conformers **a** and **b** in CDCl_3 and $\text{DMSO}-d_6$.

Compound	Solvent	Functional group	Frequency				Assignment
			exp.		calc.		
			<i>a</i>	<i>b</i>	<i>a</i>	<i>b</i>	
1	CDCl ₃	-NH-CO-	sh.1676	1647	1730	1720	ν(C=O)
		-C=N-	1603	-	1608	1616	ν(C=N)
		-C=C-	1627	-	1650	1687	ν(C=C)
		-NH	3438	3356	3569	3519	ν(N-H)
1	DMSO- <i>d</i> ₆	-NH-CO-	1680	sh.1647	1719	1712	ν(C=O)
		-C=N-	1603	-	1616	1623	ν(C=N)
		-C=C-	1627	-	1662	1682	ν(C=C)
		-NH	3452	3381	3570	3514	ν(N-H)
2	CDCl ₃	-NH-CO-	sh.1680	1662	1734	1724	ν(C=O)
		-C=N-	1608	-	1610	1619	ν(C=N)
		-C=C-	1628	-	1647	1682	ν(C=C)
		-NH	3430	3306	3565	3519	ν(N-H)
2	DMSO- <i>d</i> ₆	-NH-CO-	1681	sh.1662	1724	1719	ν(C=O)
		-C=N-	1607	-	1618	1628	ν(C=N)
		-C=C-	1628	-	1660	1681	ν(C=C)
		-NH	3489	3438	3565	3513	ν(N-H)

Vibrational modes: ν , stretching; abbreviation sh. – shoulder.

Table 4
Activation parameters for rotational barriers of studied compounds **1** and **2** in CDCl_3 at 298 K.

Compound	Process	ΔH^\ddagger [kcal mol $^{-1}$]	ΔS^\ddagger [cal K $^{-1}$ mol $^{-1}$]	ΔG^\ddagger ^(a) [kcal mol $^{-1}$]	ΔG^\ddagger ^(b) [kcal mol $^{-1}$]
1	major \rightarrow minor	18.4(0.6)	10.6(3.0)	15.3(0.1)	14.5
	minor \rightarrow major	15.9(0.7)	3.5(2.7)	14.8(0.1)	13.5
2	major \rightarrow minor	18.9(0.7)	10.2(2.4)	15.9(0.1)	15.1
	minor \rightarrow major	19.8(0.7)	13.1(2.4)	15.8(0.1)	14.8

^(a) Values based on volume of diagonal and cross peaks in VT ^1H EXSY NMR spectra. Quoted errors in parentheses combine either the statistical errors based on scattering of the data points around Eyring straight line, or the errors computed using error propagation equations (see the experimental part for details).

^(b) Theoretical calculations of effective ΔG^\ddagger (taking into account the rate constants through the two TS) at the B3LYP/6-31+G(d,p) level including SMD solvation model.

conformer (compare IR spectra of Fig. 9S and 10S). This band has also a shoulder at 1662 cm^{-1} , which may be attributed to the presence of **2b** conformer. However, this can be accompanied by the breakdown of the molecular association by alcohol (H_2O) in $\text{DMSO}-d_6$ solution. We should note that the $\nu(\text{N}-\text{H})$ stretching mode is shifted to low frequency at 3381 cm^{-1} , which may due to a H-bond because the S=O group of $\text{DMSO}-d_6$ may form the intermolecular hydrogen bonds with N-H of the amide group. The $\nu(\text{C}=\text{N})$ stretching vibrations of the C=N group and those of the conjugated double bond $\nu(\text{C}=\text{C})$ are not influenced significantly by the solvent change (see Table 3).

IR analysis of **1** and **2** indicates that there is more than one conformer in solution. However its identification is hampered by the presence of H-bonds between target compounds and small residuals of H_2O and alcohol in the solvents used in our measurements.

3.3. NMR study of compounds **1** and **2** in CDCl_3 and $\text{DMSO}-d_6$

^1H NMR spectra of compounds **1** and **2** in CDCl_3 reveal dynamic behavior. Three possible pathways could be responsible for the respective fluxionality of the compounds (Scheme 1). The first mechanism is C=N double bond isomerization, which would lead to *E/Z* exchange around C=N double bond. The second one is an amide rotation, which will produce *syn/antiperiplanar* conformers around the amide CO-NH bond. The third one is hindered rotation around the N-N bond, producing *syn/antiperiplanar* conformers. All possible species are eight (notation **a-h** in Scheme 1). The theoretical calculations in CDCl_3 at B3LYP/6-31+G(d,p) and MP2/6-31+G(d,p) levels of theory reveal the assignment of observed major

conformer in NMR spectra as (*E*)-*anti,anti* (notation **a**) and minor conformer as (*E*)-*syn, anti* (notation **b**). The thermodynamic stabilities of the other six conformers are more than 2 kcal mol $^{-1}$ less than the stability of conformer **a** and therefore their population in solution is insignificant. The experimental NOESY spectra of both compounds **1** and **2** in CDCl_3 show NOE cross peaks between NMR signals of the following atom pairs (H-4 and H-9, H-9 and NH, NH and H-2'/H-6'), which is in accordance with the above assignment of major and minor conformers in NMR spectra. According to the available literature data [12,32] the most stable isomers are *E* around C=N double bond and the antiperiplanar one around the amide CO-NH bond. According to recent X-ray data [8], the configuration of compounds **1** and **2** in solid state is (*E*)-*anti,anti* (notation **a**). Selected experimental (X-ray) and calculated bond lengths of the studied compounds **1** and **2** are presented in Table 5. Although the experimental data are for solid state and the

Table 5
Selected experimental (X-ray) and calculated bond distances for studied compounds **1** and **2**. For numbering of the atoms see Fig. 1.

Bond distance (Å)	1 ^(a)	1a ^(b)	1a ^(c)	2 ^(a)	2a ^(b)	2a ^(c)
N-N	1.380(5)	1.365	1.367	1.384(3)	1.367	1.370
N-C10	1.380(5)	1.374	1.371	1.332(4)	1.369	1.367
N=C9	1.284(6)	1.293	1.304	1.266(4)	1.294	1.302
C10=O	1.232(6)	1.232	1.240	1.226(3)	1.231	1.239
O-C8A	1.372(6)	1.365	1.379	1.370(4)	1.365	1.379
O-C2	1.452(5)	1.458	1.457	1.445(3)	1.458	1.457

^(a) X-ray data.

^(b) SMD//B3LYP/6-31+G(d,p) calculations in DMSO .

^(c) C-PCM/MP2/6-31+G(d,p) calculations in DMSO .

presented theoretical data are for DMSO solution and they cannot be compared directly, there is a very good agreement between the experimental and theoretical structural parameters in Table 5.

2D EXSY spectra were obtained to evaluate the observed exchange process. The rate constants for all compounds were determined by qualitative estimation of detected chemical exchange using raw volume intensities of diagonal and cross peaks for H-2 signals, in the 5.2–5.8 ppm range, in 2D EXSY spectra in CDCl₃ at various temperatures (Fig. 1S, 2S and 4S and 5S). These signals were chosen because they are very sensitive to the chemical exchange, don't overlap with other signals and can be integrated precisely. The activation thermodynamic parameters (ΔG^\ddagger , ΔH^\ddagger and ΔS^\ddagger) were calculated from determined temperature dependence of rate constants applying the Eyring equation. Linear dependences of $\ln(k/T)$ vs $1000/T$ for all studied complexes showed R^2 values in range from 0.9999 to 0.9992 that showed reasonable precision of collected experimental data (Figs. 3S and 6S). The barriers of isomerization, ΔG^\ddagger , are in the range of 14.8–15.9 kcal mol⁻¹, and are in the range of typical rotational barriers for amide systems [33,34].

4. Conclusion

The conformational investigation of hydrazine derivatives bearing chromene moiety was performed using theoretical (*ab initio* and DFT) and experimental (dynamic NMR and IR spectroscopy) methods. The GIAO calculations at C-PCM/B3LYP/6-31+G(2d,p)//C-PCM/MP2/6-31+G(d) level in DMSO and chloroform of ¹H and ¹³C chemical shifts of studied compounds predict very well the experimental NMR data. The rotational barriers of the amide bond in the studied compounds, ΔG^\ddagger , were in the range of 14.8–15.9 kcal mol⁻¹ and were reproduced very well by DFT calculations at the SMD//B3LYP/6-31+G(d,p) level of theory. According to our theoretical and experimental results, the (*E*)-*anti*,*anti*-conformer is predominantly present in chloroform solution as well as a small amount of the (*E*)-*syn*,*anti*-conformer obtained by rotation around the amide N–NH–C=O bond. Revealing the structure, stereochemistry and conformational dynamics of hydrazine derivatives bearing chromene moiety is essential for lead optimization in drug discovery and will facilitate molecular modelling and improve docking accuracy.

Acknowledgements

The financial support by the Bulgarian National Science Fund (Projects UNA-17/2005, RNF01/0110 and DRNF-02/13) is gratefully acknowledged.

Appendix A. Supplementary data

Supplementary data to this article can be found online at <https://doi.org/10.1016/j.molstruc.2019.126880>.

References

- [1] S. Rollas, Ş.G. Küçüküzümlü, Biological activities of hydrazone derivatives, *Molecules* 12 (2007) 1910–1939.
- [2] H.N. Dogan, A. Duran, S. Rollas, G. Sener, Y. Armutak, M. Keyer-Uysal, Synthesis and structure elucidation of some new hydrazones and oxadiazolines: anticonvulsant activities of 2-(3-acetyloxy-2-naphthyl)-4-acetyl-5-substituted-1,3,4-oxadiazolines, *Med. Sci. Res.* 26 (1998) 755–758.
- [3] R. Kalsi, M. Shrimali, T.N. Bhalla, J.P. Barthwal, Synthesis and anti-inflammatory activity of indolyl azetidinones, *Indian J. Pharm. Sci.* 52 (1990) 129–134.
- [4] R.M. Mohareb, D.H. Fleita, O.K. Sakka, Novel synthesis of hydrazide-hydrazone derivatives and their utilization in the synthesis of coumarin, pyridine, thiazole and thiophene derivatives with antitumor activity, *Molecules* 16 (2011) 16–27.
- [5] L. Popiolek, A. Biernasiuk, Hydrazone-hydrazones of 3-methoxybenzoic acid and 4-tert-butylbenzoic acid with promising antibacterial activity against *Bacillus* spp, *J. Enzym. Inhib. Med. Chem.* 31 (2016) 62–69.
- [6] L. Popiolek, Hydrazide-hydrazones as potential antimicrobial agents: overview of the literature since 2010, *Med. Chem. Res.* 26 (2017) 287–301.
- [7] V. Velezheva, P. Brennan, P. Ivanov, A. Kornienko, S. Lyubimov, K. Kazarian, B. Nikonenko, K. Majorov, A. Apt, Synthesis and antituberculous activity of indole-pyridine derived hydrazides, hydrazide-hydrazones, and thio-semicarbazones, *Bioorg. Med. Chem. Lett* 26 (2016) 978–985.
- [8] V.T. Angelova, V. Valcheva, T. Pencheva, Y. Voynikov, N. Vassilev, R. Mihaylova, G. Momekov, B. Shivachev, Synthesis, antimycobacterial activity and docking study of 2-aryl-[1]benzopyrano[4,3-c]pyrazol-4(1H)-one derivatives and related hydrazide-hydrazones, *Bioorg. Med. Chem. Lett* 27 (2017) 2996–3002.
- [9] V.T. Angelova, N.G. Vassilev, B. Nikolova-Mladenova, J. Vitas, R. Malbaša, G. Momekov, M. Djukic, L. Saso, Antiproliferative and antioxidative effects of novel hydrazone derivatives bearing coumarin and chromene moiety, *Med. Chem. Res.* (2016) 1–11.
- [10] V.T. Angelova, Y. Voynikov, P. Andreeva-Gateva, S. Surcheva, N. Vassilev, T. Pencheva, J. Tchekalarova, In vitro and in silico evaluation of chromene based aryl hydrazones as anticonvulsant agents, *Med. Chem. Res.* 26 (2017) 1884–1896.
- [11] V. Angelova, V. Karabeliov, P.A. Andreeva-Gateva, J. Tchekalarova, Recent developments of hydrazide/hydrazone derivatives and their analogs as anticonvulsant agents in animal models, *Drug Dev. Res.* 77 (2016) 379–392.
- [12] A.B. Lopes, E. Miguez, A.E. Kümmerle, V.M. Rumjanek, C.A.M. Fraga, E.J. Barreiro, Characterization of amide bond conformers for a novel heterocyclic template of N-acylhydrazone derivatives, *Molecules* 18 (2013) 11683–11704.
- [13] M.J. Frisch, G.W. Trucks, H.B. Schlegel, G.E. Scuseria, M.A. Robb, J.R. Cheeseman, G. Scalmani, V. Barone, B. Mennucci, G.A. Petersson, H. Nakatsuji, M. Caricato, X. Li, H.P. Hratchian, A.F. Izmaylov, J. Bloino, G. Zheng, J.L. Sonnenberg, M. Hada, M. Ehara, K. Toyota, R. Fukuda, J. Hasegawa, M. Ishida, T. Nakajima, Y. Honda, O. Kitao, H. Nakai, T. Vreven, J.A. Montgomery Jr., J.E. Peralta, F. Ogliaro, M. Bearpark, J.J. Heyd, E. Brothers, K.N. Kudin, V.N. Staroverov, R. Kobayashi, J. Normand, K. Raghavachari, A. Rendell, J.C. Burant, S.S. Iyengar, J. Tomasi, M. Cossi, N. Rega, J.M. Millam, M. Klene, J.E. Knox, J.B. Cross, V. Bakken, C. Adamo, J. Jaramillo, R. Gomperts, R.E. Stratmann, O. Yazyev, A.J. Austin, R. Cammi, C. Pomelli, J.W. Ochterski, R.L. Martin, K. Morokuma, V.G. Zakrzewski, G.A. Voth, P. Salvador, J.J. Dannenberg, S. Dapprich, A.D. Daniels, Ö. Farkas, J.B. Foresman, J.V. Ortiz, J. Cioslowski, D.J. Fox, Gaussian 09, Revision D.01, Gaussian, Inc., Wallingford CT, 2009.
- [14] A.D. Becke, Density-functional thermochemistry. III. The role of exact exchange, *J. Chem. Phys.* 98 (1993) 5648–5652.
- [15] C.T. Lee, W.T. Wang, R.G. Pople, Development of the Colle-Salvetti correlation-energy formula into a functional of the electron density, *Phys. Rev. B* 37 (1988) 785–789.
- [16] A.V. Marenich, C.J. Cramer, D.G. Truhlar, Universal solvation model based on solute electron density and on a continuum model of the solvent defined by the bulk dielectric constant and atomic surface tensions, *J. Phys. Chem. B* 113 (2009) 6378–6396.
- [17] M. Cossi, N. Rega, G. Scalmani, V. Barone, Energies, structures, and electronic properties of molecules in solution with the C-PCM solvation model, *J. Comput. Chem.* 24 (2003) 669–681.
- [18] J. Tomasi, B. Mennucci, R. Cammi, Quantum mechanical continuum solvation models, *Chem. Rev.* 105 (2005) 2999–3093.
- [19] R. Ditchfield, Self-consistent perturbation theory of diamagnetism, *Mol. Phys.* 27 (1974) 789–807.
- [20] K. Wolinski, J.F. Hinton, P. Pulay, Efficient implementation of the gauge-independent atomic orbital method for NMR chemical shift calculations, *J. Am. Chem. Soc.* 112 (1990) 8251–8260.
- [21] G.S. Kottas, L.I. Clarke, D. Horinek, J. Michl, Artificial molecular rotors, *Chem. Rev.* 105 (2005) 1281–1376.
- [22] D. Enders, H. Gielen, Synthesis of chiral triazolinyldene and imidazolinyldene transition metal complexes and first application in asymmetric catalysis, *J. Organomet. Chem.* 617–618 (2001) 70–80.
- [23] J.C. Bernhammer, H.V. Huynh, Nickel(II) benzimidazolin-2-ylidene complexes with thioether-functionalized side chains as catalysts for suzuki–miyaura cross-coupling, *Organometallics* 33 (2014) 5845–5851.
- [24] E.W. Abel, T.P.J. Coston, K.G. Orrell, V. Šik, D. Stephenson, Two-dimensional NMR exchange spectroscopy. Quantitative treatment of multisite exchanging systems, *J. Magn. Reson.* 70 (1969) 34–53, 1986.
- [25] L.M. Jackman, F.A. Cotton, R.D. Adams, Dynamic Nuclear Magnetic Resonance Spectroscopy, Academic Press, New York, 1975.
- [26] J. Heinzer, J.F.M. Oth, Iterative least-squares lineshape fitting of H-1-Decoupled C-13-Dnmr spectra, *Helv. Chim. Acta* 64 (1981) 258–278.
- [27] H. Valdés, D. Reha, P. Hobza, Structure of isolated tryptophyl-glycine dipeptide and tryptophyl-glycyl-glycine tripeptide: ab initio SCC-DFTB-D molecular dynamics simulations and high-level correlated ab initio quantum chemical calculations, *J. Phys. Chem. B* 110 (2006) 6385–6396.
- [28] T. Van Mourik, P.G. Karamertzanis, S.L. Price, Molecular conformations and relative stabilities can be as demanding of the electronic structure method as intermolecular calculations, *J. Phys. Chem. A* 110 (2006) 8–12.
- [29] S.C.C. Nunes, A.J.L. Jesus, M.T.S. Rosado, M.E.S. Eusebio, Conformational study of isolated pindolol by HF, DFT and MP2 calculations, *J. Mol. Struct.:*

- THEOCHEM 806 (2007) 231–238.
- [30] R.A. Russell, H.W. Thompson, Vibrational spectra and geometrical isomerism in amides, *Spectrochim. Acta* 8 (1956) 138–141.
- [31] H.E. Hallam, C.M. Jones, Conformational isomerism of the amide group - a review of the IR and NMR spectroscopic evidence, *J. Mol. Struct.* 5 (1970) 1–19.
- [32] H.A. Abdel-Aziz, H.A. Ghabbour, W.M. Eldehna, M.M. Qabeel, H.K. Fun, Synthesis, crystal structure, and biological activity of cis/trans amide rotomers of (Z)- N'-(2-Oxoindolin-3-ylidene)formohydrazide, *J. Chem.* (2014) 2014.
- [33] W.E. Stewart, T.H. Siddall III, Nuclear magnetic resonance studies of amides, *Chem. Rev.* 70 (1970) 517–551.
- [34] K.B. Wiberg, P.R. Rablen, D.J. Rush, T.A. Keith, Amides. 3. Experimental and theoretical studies of the effect of the medium on the rotational barriers for n, n-dimethylformamide and n, n-dimethylacetamide, *J. Am. Chem. Soc.* 117 (1995) 4261–4270.